

## Supporting Information

### Near-Infrared Absorption by Intramolecular Charge Transfer Transition in 5,10,15,20-Tetra(*N*-carbazolyl)porphyrin through Protonation

Shin-ichiro Kawano,<sup>†</sup> Sae Kawada,<sup>†</sup> Yasutaka Kitagawa,<sup>‡</sup> Rena Teramoto,<sup>‡</sup> Masayoshi Nakano,<sup>‡</sup> and Kentaro Tanaka<sup>\*,†</sup>

<sup>†</sup>*Department of Chemistry, Graduate School of Science,  
Nagoya University, Furocho, Chikusa-ku, Nagoya 464-8602 (Japan)*

<sup>‡</sup>*Division of Chemical Engineering, Department of Materials Engineering Science, Graduate School of Science, Osaka  
University, 1-3 Machikaneyama-cho, Toyonaka, Osaka, 560-8531 (Japan)*

*E-mail: kentaro@chem.nagoya-u.ac.jp*

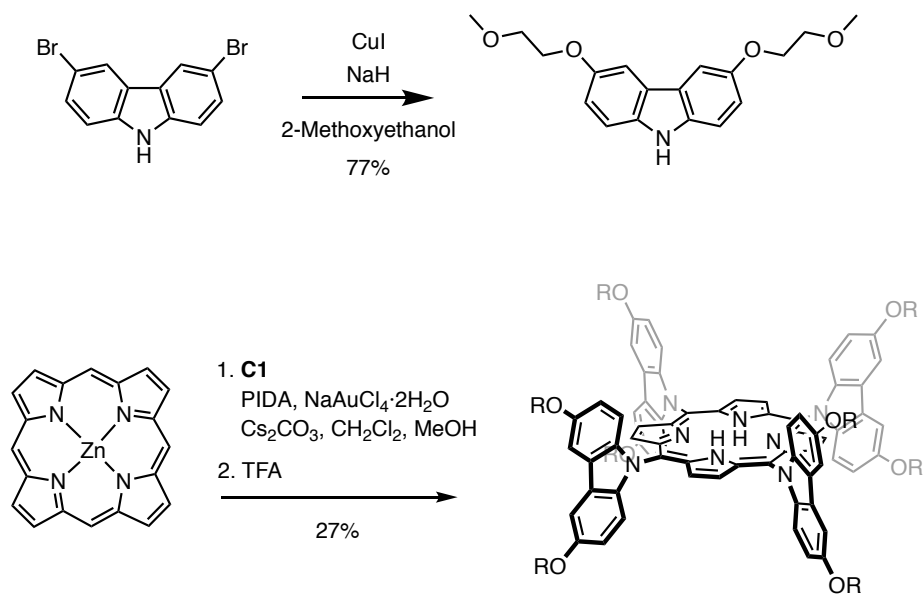
### Contents

1.	Experimental	p. S2
2.	Synthesis	p. S3
3.	X-ray crystallographic analysis of H <sub>2</sub> P1 and H <sub>4</sub> P1 <sup>2+</sup>	p. S9
4.	Absorption and fluorescence spectra of H <sub>2</sub> P1	p. S15
5.	DPV of H <sub>2</sub> P1	p. S16
6.	Photometric titration of trifluoromethanesulfonic acid against H <sub>2</sub> P1 and H <sub>2</sub> TPP	p. S17
7.	Theoretical calculations	p. S18
8.	References	p. S21

## 1. Experimental

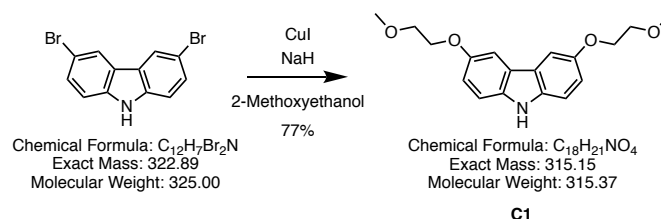
Synthetic procedures were carried out under dry nitrogen atmosphere, unless otherwise specified. All of the chemicals were purchased at the highest commercial quality available (Wako, Kanto, TCI, and Aldrich) and used without any further purification, unless otherwise stated. The syntheses of Zn-porphine were reported previously.<sup>1</sup>  $^1\text{H}$  and  $^{13}\text{C}$  NMR spectra were recorded on a JNM-ECS400 (400 MHz for  $^1\text{H}$ ; 100 MHz for  $^{13}\text{C}$ ) and JNM-ECA600 (600 MHz for  $^1\text{H}$ ; 150 MHz for  $^{13}\text{C}$ ) spectrometers at a constant temperature of 298 K. Tetramethylsilane (TMS) was used as an internal reference for  $^1\text{H}$  and  $^{13}\text{C}$  NMR measurements in  $\text{CDCl}_3$ . Elemental analyses were performed on a Yanaco MT-6 analyzer. Silica gel column chromatography was performed using Merck silica gel 60. GPC was performed using a JAI LC-9204 equipped with JAIGEL 2H-40/1H-40 or 3H-40/2.5H-40 columns. ESI-TOF Mass spectroscopy was performed with a micrOTOF-QII, Bruker. Matrix-assisted laser desorption ionization time-of-flight mass spectroscopy (MALDI-TOF-MS) was performed with an ultraflex III, Bruker Daltonics and dithranol was used as the matrix. The absorption spectra were recorded with a Hitachi U-4100 spectrophotometer in  $\text{CHCl}_3$  solutions at  $20 \pm 0.1$  °C in 1.0 cm quartz cells. The fluorescence spectra were measured with a Hitachi F-4500 fluorescence spectrophotometer in  $\text{CHCl}_3$  solutions at  $20 \pm 0.1$  °C in 1.0 cm quartz cells. Cyclic voltammetry (CV) and the differential-pulse voltammetry (DPV) were conducted using a BAS Electrochemical Analyzer Model ALS 750 Ds. The CV cell consisted of a glassy carbon electrode as a working electrode, a Pt wire as a counter electrode, and a  $\text{Ag}/\text{AgCl}$  in  $\text{CH}_3\text{CN}$  as a reference electrode. Tetrabutylammonium hexafluorophosphate was used as a supporting electrolyte. The redox potentials were calibrated with ferrocene as an internal standard.

## 2. Synthesis



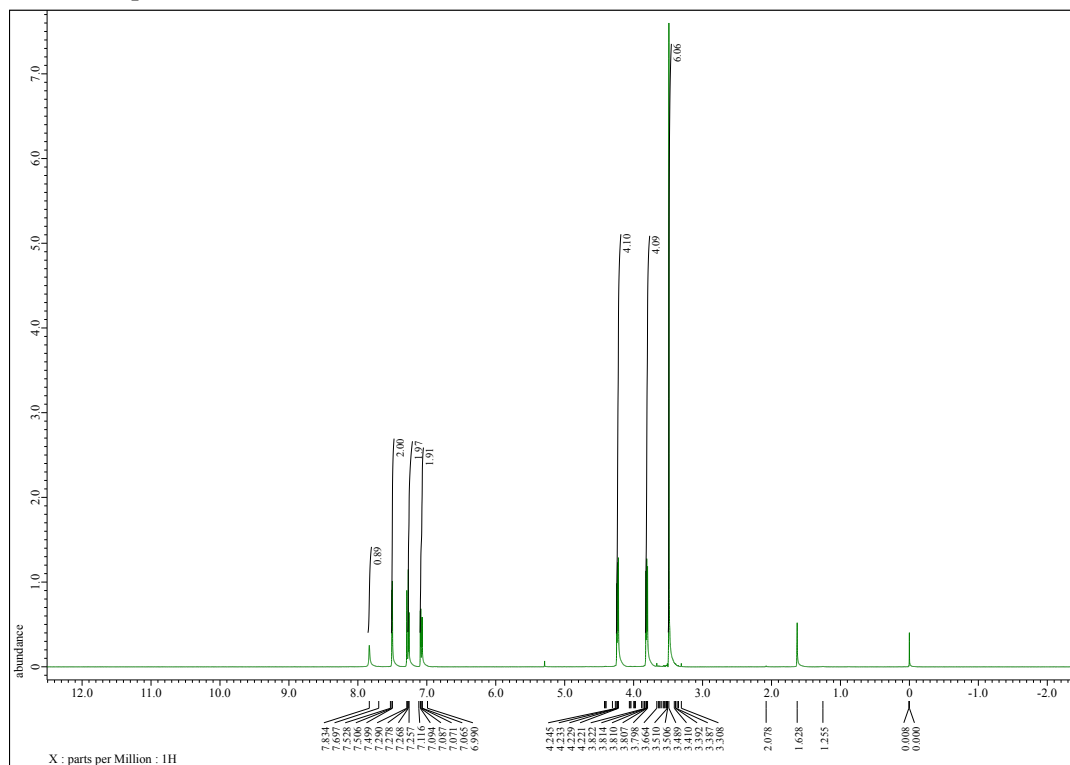
**Scheme S1.** Synthesis of 5,10,15,20-tetra(*N*-carbazolyl)porphyrin

## 2-1. Synthesis of 3,6-di(2-methoxyethoxy)carbazole, **C1**

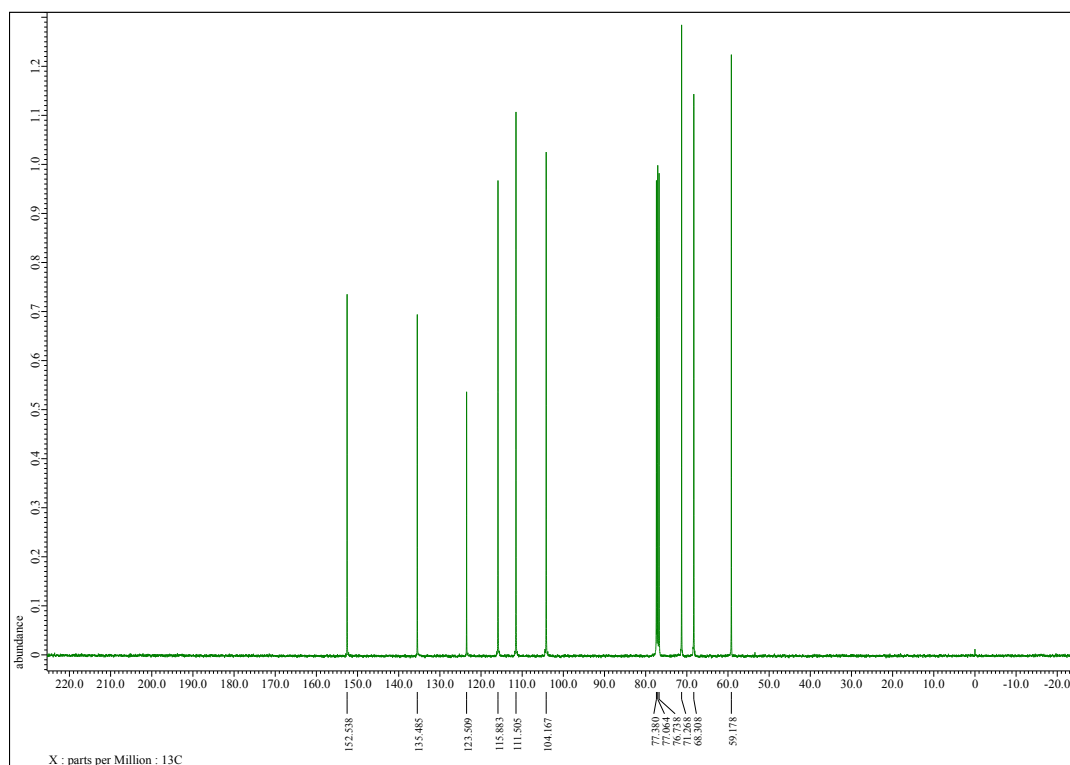


NaH (24.4 g, 614 mmol, 20 equiv.) was dissolved in 2-methoxyethanol (350 mL). 3,6-Dibromocarbazole (10.1 g, 30.7 mmol) and CuI (24.3 g, 129 mmol) were added to the solution. The mixture was refluxed for 19 h. After cooling, the reaction mixture was filtered to remove insoluble inorganic materials. The residue was washed with AcOEt. The filtrate was washed with 10% Na<sub>2</sub>S<sub>2</sub>O<sub>3</sub> solution (500 mL × 1), water (500 mL × 3), brine (500 mL × 1). The organic layer was collected and dried with anhydrous Na<sub>2</sub>SO<sub>4</sub>, then evaporated to obtain brown solid and colorless liquid. The colorless liquid was removed with decantation to obtain crude as brown solid. The crude was purified by SiO<sub>2</sub> column chromatography (SiO<sub>2</sub>, hexane: AcOEt = 5:1-3:1) to obtain **C1** as colorless solid (7.48 g, 77%). <sup>1</sup>H NMR (400 MHz, CDCl<sub>3</sub>/TMS) δ = 7.82 (s, 1H), 7.51-7.50 (d, *J* = 2.4 Hz, 2H), 7.30-7.26 (m, 2H), 7.10-7.07 (d-d, *J* = 2.4 Hz, 8.6 Hz, 2H), 4.25-4.22 (t, *J* = 4.8, 4H), 3.82-3.80 (t, *J* = 4.8, 4H), 3.49 (s, 6H), <sup>13</sup>C NMR (100 MHz, CDCl<sub>3</sub>/TMS) δ = 152.5, 135.5, 123.5, 115.9, 111.5, 104.2, 71.3, 68.3, 59.2. HRMS (ESI-TOF) *m/z*: [M + Na]<sup>+</sup> Calcd for C<sub>18</sub>H<sub>21</sub>NO<sub>4</sub>Na 338.1368; Found 338.1365. IR (ATR): 3314 (NH), 1204 (ArOR), 1046 (ArOR) cm<sup>-1</sup>.

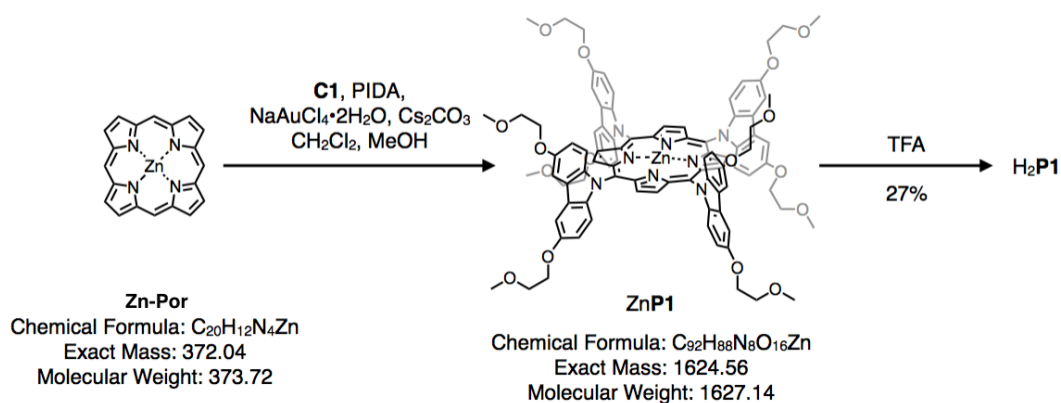
$^1\text{H}$  NMR spectrum of **C1**



$^{13}\text{C}$  NMR spectrum of **C1**

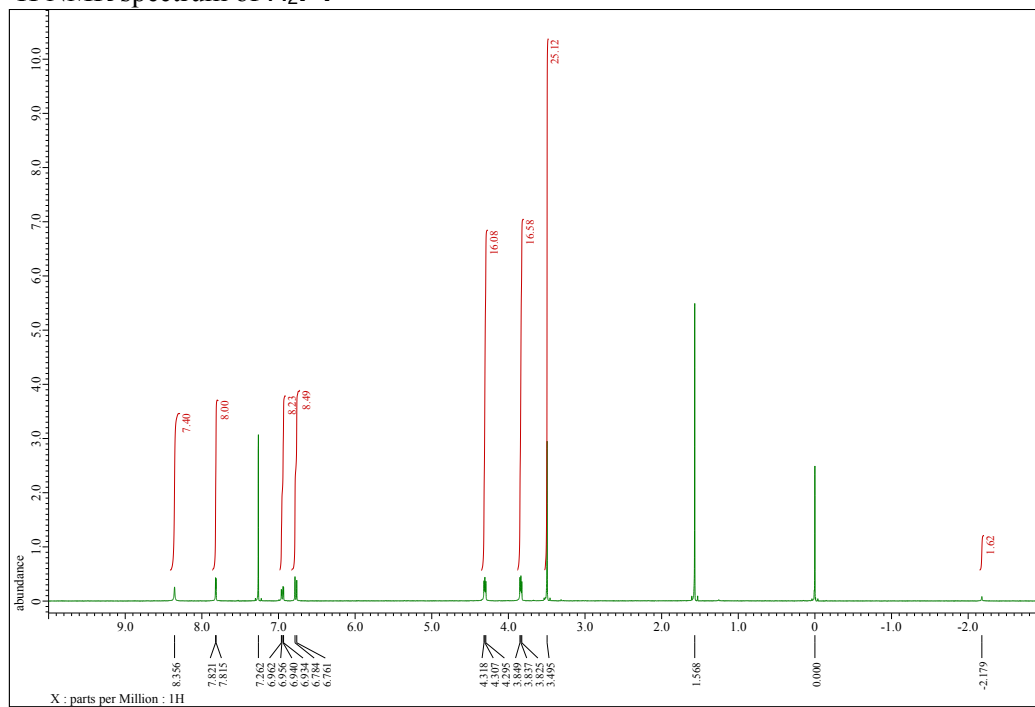


## Synthesis of H<sub>2</sub>P1

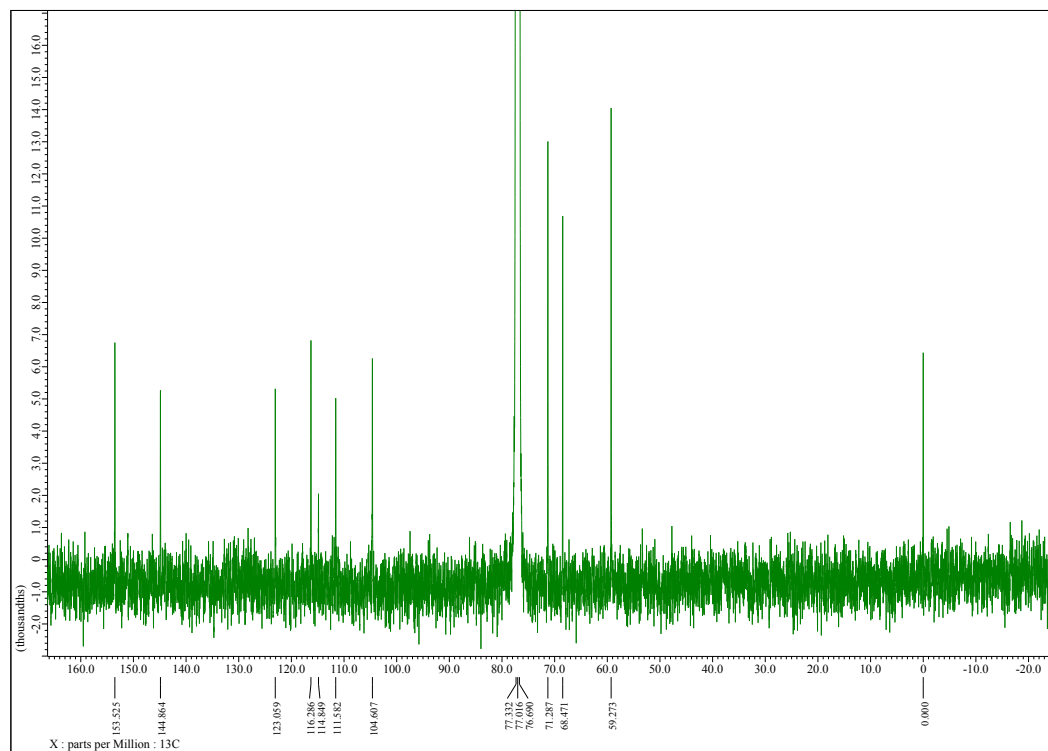


**Zn-por**<sup>1</sup> (32.2 mg, 80.3  $\mu$ mol) and **C1** (257 mg, 803  $\mu$ mol) were dissolved in dry CH<sub>2</sub>Cl<sub>2</sub> (160 mL) and MeOH (5 mL). Cs<sub>2</sub>CO<sub>3</sub> (0.537 g, 1.6 mmol, 20 equiv) was added to the solution. To the stirred solution of **Zn-por** and **C1**, phenyliondine diacetate: PIDA (108 mg, 241  $\mu$ mol, 4 equiv) and NaAuCl<sub>4</sub>·2H<sub>2</sub>O (192 mg, 482  $\mu$ mol, 6 equiv) were added. The reaction mixture was stirred at room temperature for 30 min. The reaction was quenched with 10% Na<sub>2</sub>S<sub>2</sub>O<sub>4</sub> aqueous solution 200 mL, then reaction mixture was filtered. The organic layer was collected and washed with 10% Na<sub>2</sub>S<sub>2</sub>O<sub>4</sub> aqueous solution (200 mL), water (200 mL  $\times$  2), brine (200 mL), and dried over anhydrous Na<sub>2</sub>SO<sub>4</sub>, then evaporated to obtain brown solid. The solid was dissolved in CH<sub>2</sub>Cl<sub>2</sub> (20 mL) and MeOH (5 mL). TFA (6.40 mL, 83.6 mmol) was added to the solution. The solution was stirred at room temperature for 1 h. 1M NaOH aqueous solution (200 mL) and CH<sub>2</sub>Cl<sub>2</sub> (150 mL) were added to the solution. The organic layer was collected and washed with sat. NaHCO<sub>3</sub> aqueous solution (200 mL), water (200 mL  $\times$  2), brine (200 mL), dried over anhydrous Na<sub>2</sub>SO<sub>4</sub>, then evaporated to obtain crude. The crude was SiO<sub>2</sub> column chromatography (3.5 cm $\phi$   $\times$  10 cm, CH<sub>2</sub>Cl<sub>2</sub>: MeOH = 100:1, 50:1) to obtain the fraction containing the target. This fraction was further purified by GPC (JAIGEL, 2H-1H, eluent: CHCl<sub>3</sub>) to obtain the target as brown solid (34.3 mg, 21.8  $\mu$ mol, 27%). <sup>1</sup>H NMR (400 MHz, CDCl<sub>3</sub>/TMS)  $\delta$  = 8.36 (s, 8H), 7.82–7.81 (d,  $J$  = 2.4 Hz, 8H), 6.96–6.93 (d-d,  $J$  = 2.4 Hz, 9.2, 8H), 6.78–6.76 (d,  $J$  = 9.2 Hz, 8H), 4.32–4.29 (t,  $J$  = 4.4 Hz, 16H), 3.85–3.82 (t,  $J$  = 4.4 Hz, 16H) 3.49 (s, 24H), –2.17 (s, 2H). <sup>13</sup>C NMR (100 MHz, CDCl<sub>3</sub>/TMS)  $\delta$  = 153.5, 144.9, 123.1, 116.3, 114.8, 111.6, 104.6, 71.3, 68.5, 59.3. MALDI-TOF MS (dithranol, positive);  $m/z$  calcd for [M + H]<sup>+</sup> 1563.7 found 1563.9, Anal. calcd for C<sub>92</sub> H<sub>90</sub> N<sub>8</sub> O<sub>8</sub>·0.2CHCl<sub>3</sub>. C 69.75 H 5.73 N 7.06; found C 69.86 H 5.81 N 6.76. IR (ATR): 1200 (ArOR), 1026 (ArOR) cm<sup>-1</sup>.

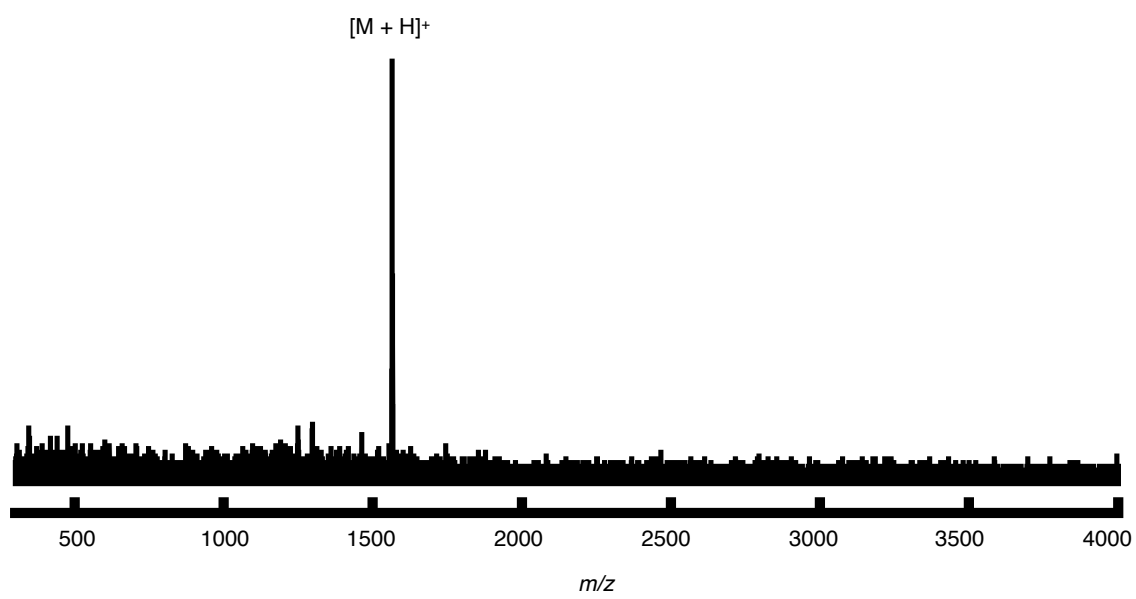
$^1\text{H}$  NMR spectrum of  $\text{H}_2\text{P1}$



$^{13}\text{C}$  NMR spectrum of  $\text{H}_2\text{P1}$



MALDI TOF-MS of H<sub>2</sub>P1



### 3. X-ray crystallographic analysis of H<sub>2</sub>P1 and H<sub>4</sub>P1<sup>2+</sup>

#### 3-1. X-ray crystallographic analysis of H<sub>2</sub>P1

Single crystal X-ray diffraction measurement was performed with a Rigaku X-ray diffractometer equipped with a molybdenum MicroMax-007 and Saturn 70 CCD detector. The structure was solved by the direct method (SHELXL-2014) and refined by the full-matrix least-squares on  $F^2$  (SHELXL-2014/6) using Yadokari-XG 2014.<sup>2</sup> All non-hydrogen atoms were refined anisotropically.

Red crystals of H<sub>2</sub>P1 suitable for X-ray analysis were obtained by slow vapor diffusion of methanol into CHCl<sub>3</sub> at room temperature. The measurement was performed at 123 K. Total 39056 reflections were collected, among which 8045 reflections were independent ( $R_{\text{int}} = 0.0386$ ). The crystal data are deposited in the Cambridge Crystallographic Data Centre (CCDC 1864209). The crystal data are as follows: Formula C<sub>92</sub>H<sub>90</sub>N<sub>8</sub>O<sub>16</sub>; FW = 1563.71, crystal size 0.35 × 0.35 × 0.1 mm<sup>3</sup>, monoclinic, space group  $P2_1/a$  (#14),  $a = 13.051(14)$  Å,  $b = 18.73(2)$  Å,  $c = 19.67(2)$  Å,  $\alpha = 90^\circ$ ,  $\beta = 90.899(10)^\circ$ ,  $\gamma = 90^\circ$ ,  $V = 4808(9)$  Å<sup>3</sup>,  $Z = 2$ ,  $D_{\text{calcd}} = 1.080$  g cm<sup>-3</sup>;  $R_1 = 0.0789$  ( $I > 2(I)$ ),  $wR_2 = 0.2270$  (all data),  $GOF = 1.089$ .

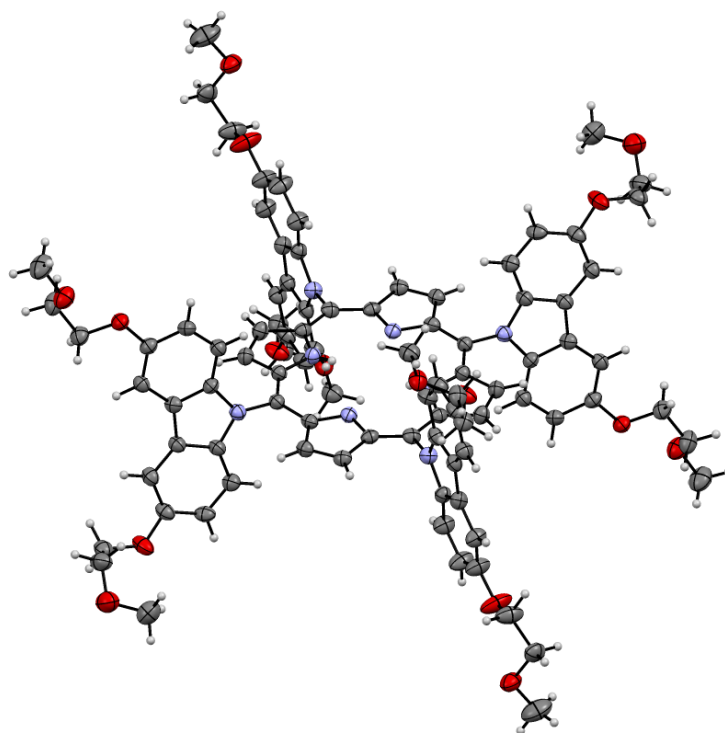


**Figure S1.** (a) Crystal structure of H<sub>2</sub>P1. ORTEP diagram with the thermal ellipsoids at a 50% probability level. Solvents were omitted for clarity.

Two methanol and two disordered chloroform were placed between the molecules in the unit cell. These solvent molecules were removed using the ‘SQUEEZE’ procedure in the PLATON program.<sup>3</sup> The dihedral angles between carbazole and porphyrin core were 71° and 89°. In the molecular packing of H<sub>2</sub>P1, the distance between the neighboring porphyrin planes was 13 Å (Figure 1b).

**Table S1.** Identification code of H<sub>2</sub>P1

Identification code	H <sub>2</sub> P1
Empirical formula	C <sub>92</sub> H <sub>90</sub> N <sub>8</sub> O <sub>16</sub>
Formula weight	1563.71
Temperature	123(2) K
Crystal system	Monoclinic
Space group	<i>P</i> 2 <sub>1</sub> /a
Unit cell dimensions	<i>a</i> = 13.051(14) Å <i>b</i> = 18.73(2) Å <i>c</i> = 19.67(2) Å <i>α</i> = 90° <i>β</i> = 90.889(10)° <i>γ</i> = 90°
Volume	4808(9) Å <sup>3</sup>
<i>Z</i>	2
Density (calcd.)	1.080 g/cm <sup>3</sup>
Absorption coefficient	0.075 mm <sup>-1</sup>
<i>F</i> (000)	1652.0
Crystal size	0.35 × 0.35 × 0.1 mm <sup>3</sup>
Goodness-of-fit on <i>F</i> <sup>2</sup>	1.089
R <sub>1</sub> [ <i>I</i> > 2s( <i>I</i> )]	0.0789
wR <sub>2</sub> [all data]	0.2270

### 3-2. X-ray crystallographic analysis of $\text{H}_4\text{P1}^{2+}\cdot 2(\text{CF}_3\text{SO}_4^-)$

Single crystal X-ray diffraction measurements were performed using synchrotron radiation ( $\lambda = 0.7004 \text{ \AA}$ ) at the BL02B1 in the SPring-8 with approval of the Japan Synchrotron Radiation Research Institute (JASRI) (proposal No. 2016B1144).

Red crystals of  $\text{H}_4\text{P1}^{2+}\cdot 2(\text{CF}_3\text{SO}_4^-)$  suitable for X-ray analysis were obtained by slow evaporation of acetonitrile at room temperature. The measurement was performed at 100 K. Total 250749 reflections were collected, among which 14618 reflections were independent ( $R_{\text{int}} = 0.0293$ ). The crystal data are deposited in The Cambridge Crystallographic Data Centre (CCDC 1868761). The crystal data are as follows: Formula  $\text{C}_{69}\text{H}_{92}\text{F}_{12}\text{N}_8\text{O}_{28}\text{S}_4$ ; FW = 2062.01, crystal size  $0.20 \times 0.20 \times 0.20 \text{ mm}^3$ , cubic, space group  $\text{P4}_32$  (#212),  $a = b = c = 33.668(2) \text{ \AA}$ ,  $\alpha = \beta = \gamma = 90^\circ$ ,  $V = 38164.7(7) \text{ \AA}^3$ ,  $Z = 12$ ,  $D_{\text{calcd}} = 1.129 \text{ g cm}^{-3}$ ;  $R_1 = 0.1133$  ( $I > 2\sigma(I)$ ),  $wR_2 = 0.3369$  (all data),  $GOF = 1.349$ .

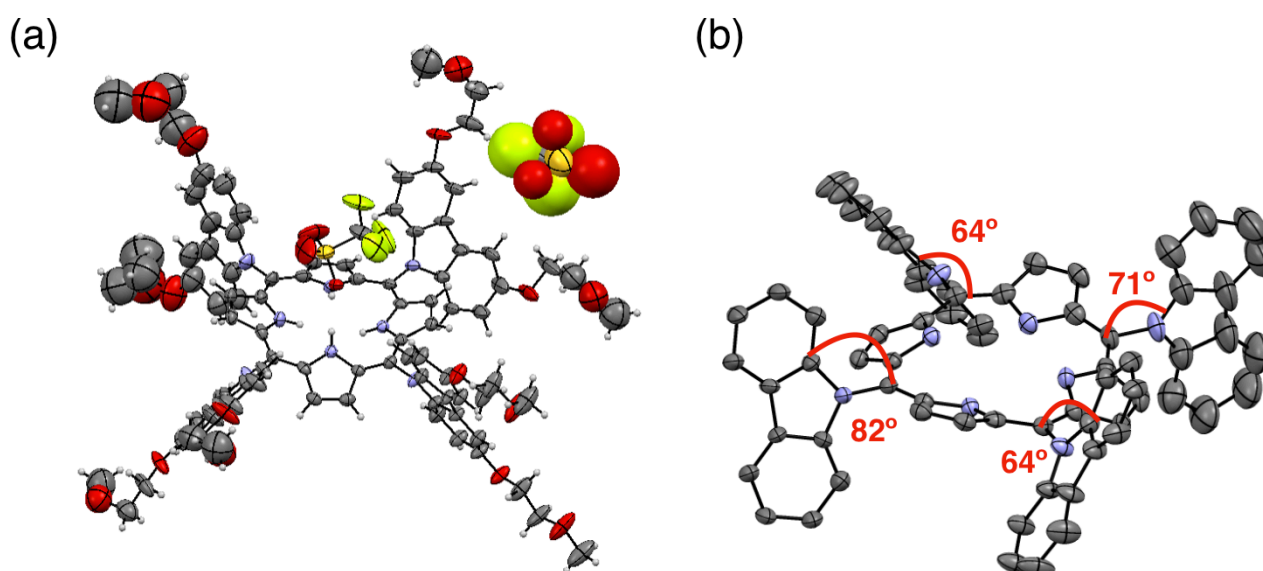


**Figure S2.** Crystal structure of  $\text{H}_4\text{P1}^{2+}\cdot 2(\text{CF}_3\text{SO}_4^-)$ . ORTEP diagram with the thermal ellipsoids at a 50% probability level. Hydrogen atoms were omitted for clarity. (b) The dihedral angles between porphyrin plane and each carbazole were shown. The side chains were omitted for clarity.

**Table S2.** Identification code of  $\text{H}_4\text{P1}^{2+}\cdot 2(\text{CF}_3\text{SO}_4^-)$ 

Identification code	$\text{H}_4\text{P1}^{2+}\cdot 2(\text{CF}_3\text{SO}_4^-)$
Empirical formula	$\text{C}_{69}\text{H}_{92}\text{F}_{12}\text{N}_8\text{O}_{28}\text{S}_4$
Formula weight	2162.01
Temperature	100(2) K
Crystal system	Cubic
Space group	$P 4_1 3 2$
Unit cell dimensions	$a = 33.668(2) \text{ \AA}$ $b = 33.668(2) \text{ \AA}$ $c = 33.668(2) \text{ \AA}$ $\alpha = 90^\circ$ $\beta = 90^\circ$ $\gamma = 90^\circ$
Volume	$38164(7) \text{ \AA}^3$
$Z$	12
Density (calcd.)	$1.129 \text{ g/cm}^3$
Absorption coefficient	$0.149 \text{ mm}^{-1}$
$F(000)$	13440
Crystal size	$0.2 \times 0.2 \times 0.2 \text{ mm}^3$
Goodness-of-fit on $F^2$	1.349
$R_1 [I > 2s(I)]$	0.1133
$wR_2 [\text{all data}]$	0.3369

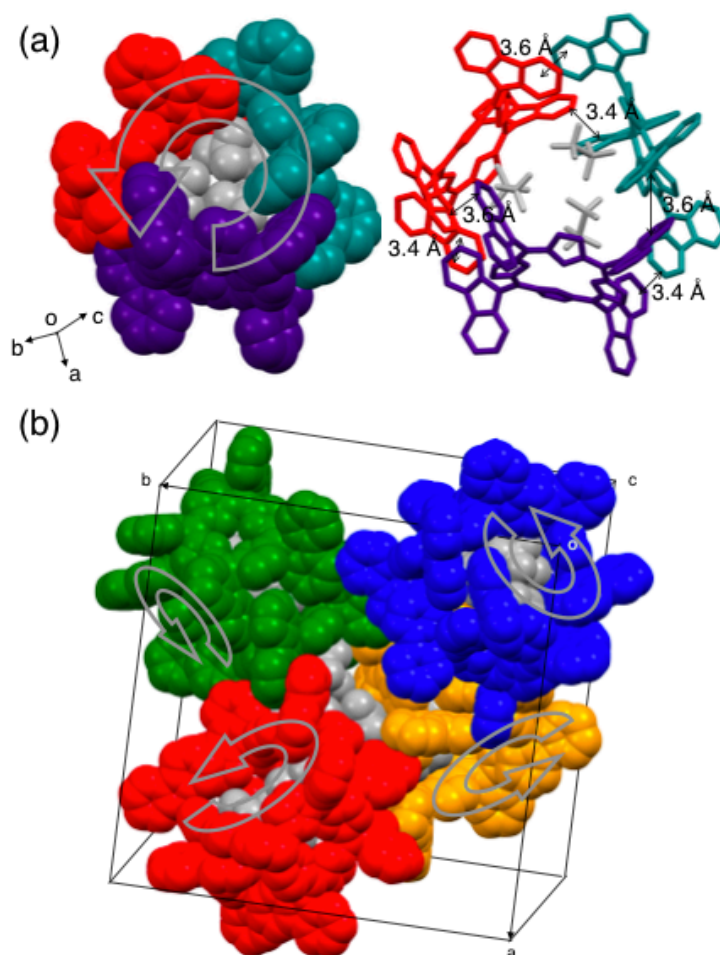


**Figure S3.** (a) Left; The packing structure of  $\text{H}_4\text{P1}^{2+}\cdot 2(\text{CF}_3\text{SO}_4^-)$  was presented with a space-filling model.  $\text{H}_4\text{P1}^{2+}$  forms the cyclic barrel-shaped trimer, in which the three counter anions,  $3\text{CF}_3\text{SO}_3^-$  were entrapped. In the crystalline structure, the cyclic trimer assembled in the chiral left-handed fashion. Right; The cyclic barrel-shaped trimer was bound through intermolecular  $\pi$ - $\pi$  interaction between the peripheral carbazoles. (b) The packing structure of  $\text{H}_4\text{P1}^{2+}\cdot 2(\text{CF}_3\text{SO}_4^-)$  in the unit cell. The four cyclic trimer were shown with different color.

There is a certain electron density due to the disordered solvent between the molecules and inside the macrocyclic structure. These solvent molecules were removed using the ‘SQUEEZE’ procedure in the PLATON program.<sup>3</sup>

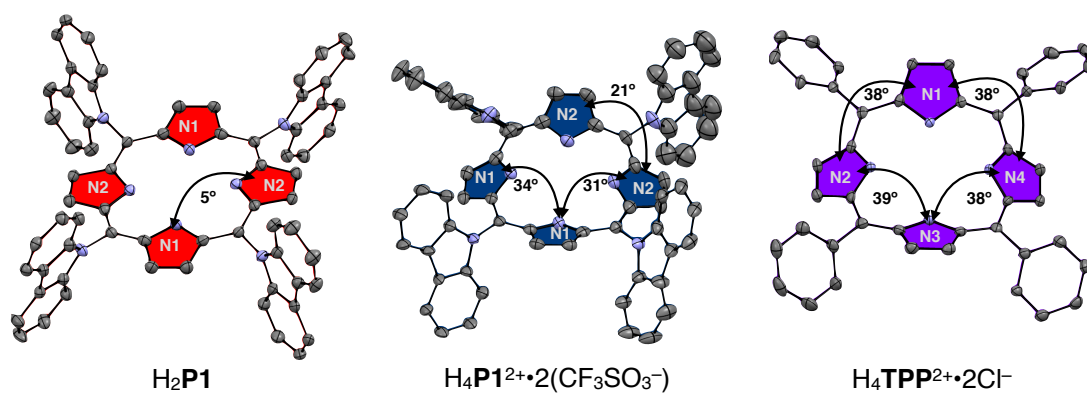


**Figure S4.** X-ray crystal structures of (a)  $\text{H}_2\text{P1}$ , (b)  $\text{H}_4\text{P1}^{2+}\cdot 2(\text{CF}_3\text{SO}_4^-)$ , and (c)  $\text{H}_4\text{TPP}^{2+}\cdot 2\text{Cl}^-$ .<sup>6</sup> The side chains and hydrogens were omitted for clarity. The plane-to-plane twist angles between the neighboring pyrrole ring of  $\text{H}_4\text{TPP}^{2+}\cdot 2\text{Cl}^-$  are  $38^\circ - 39^\circ$ .<sup>4</sup>

#### 4. Absorption and fluorescence spectra of H<sub>2</sub>P1

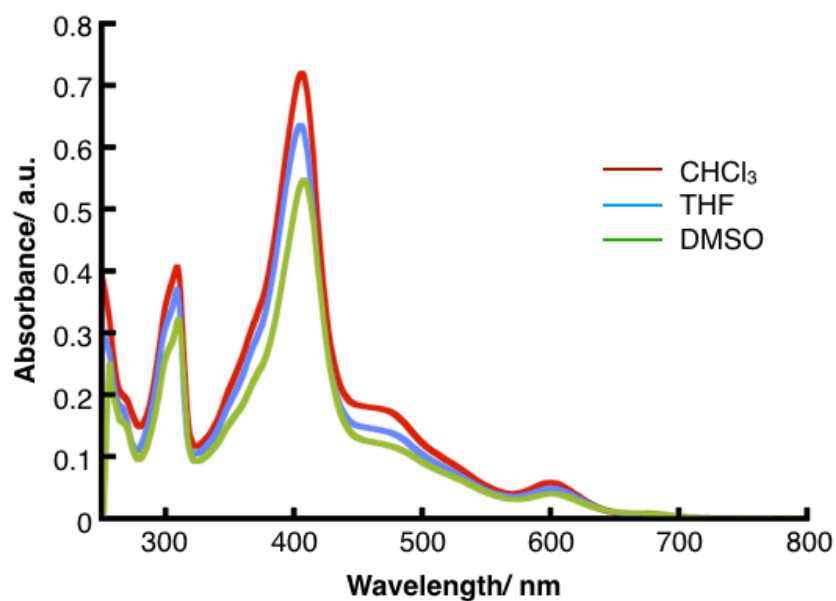


**Figure S5.** Absorption spectra of H<sub>2</sub>P1 in different solvents ([H<sub>2</sub>P1] = 5.0 μM); in CHCl<sub>3</sub> (red line), THF (blue line), and DMSO (right green line).

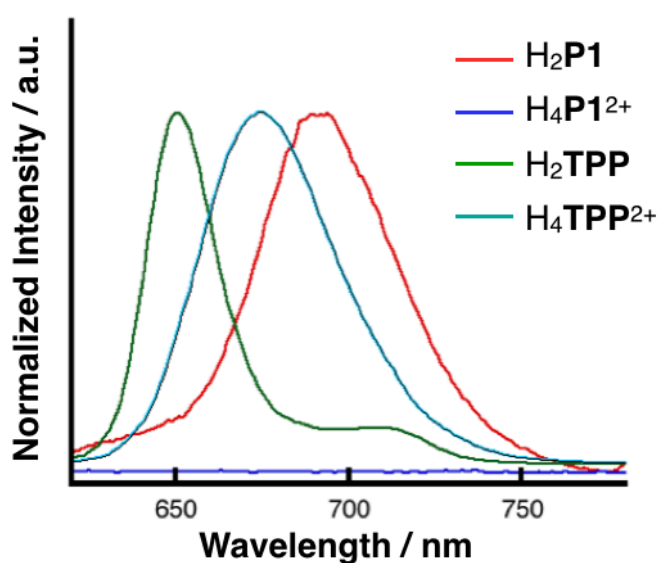


**Figure S6.** Fluorescence spectra of porphyrins in CHCl<sub>3</sub>, [porphyrin] = 0.5 μM. The fluorescence intensities for H<sub>2</sub>P1, H<sub>4</sub>P1<sup>2+</sup>, and H<sub>2</sub>TPP were normalized at the fluorescence maxima. Excitation wavelengths: 406 nm for H<sub>2</sub>P1, H<sub>4</sub>P1<sup>2+</sup>, 418 nm for H<sub>2</sub>TPP, and 438 nm for H<sub>4</sub>TPP<sup>2+</sup>.

Using the fluorescence quantum yield of H<sub>2</sub>TPP ( $\Phi_f = 0.11$ ) as a standard,<sup>5</sup> the fluorescence quantum yield of H<sub>2</sub>P1 was estimated to be 0.008.

## 5. DPV of H<sub>2</sub>P1

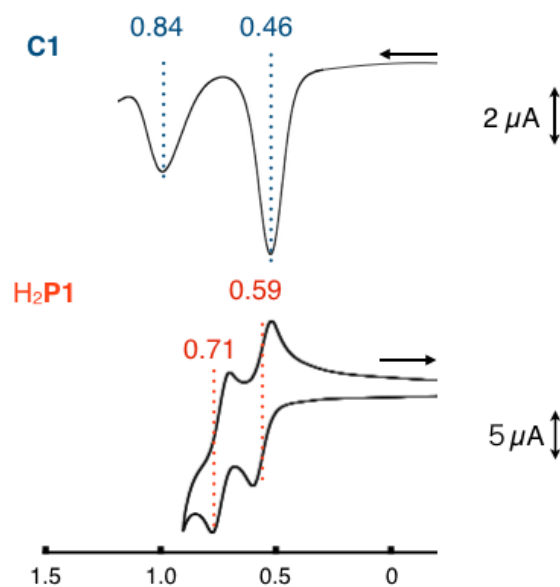


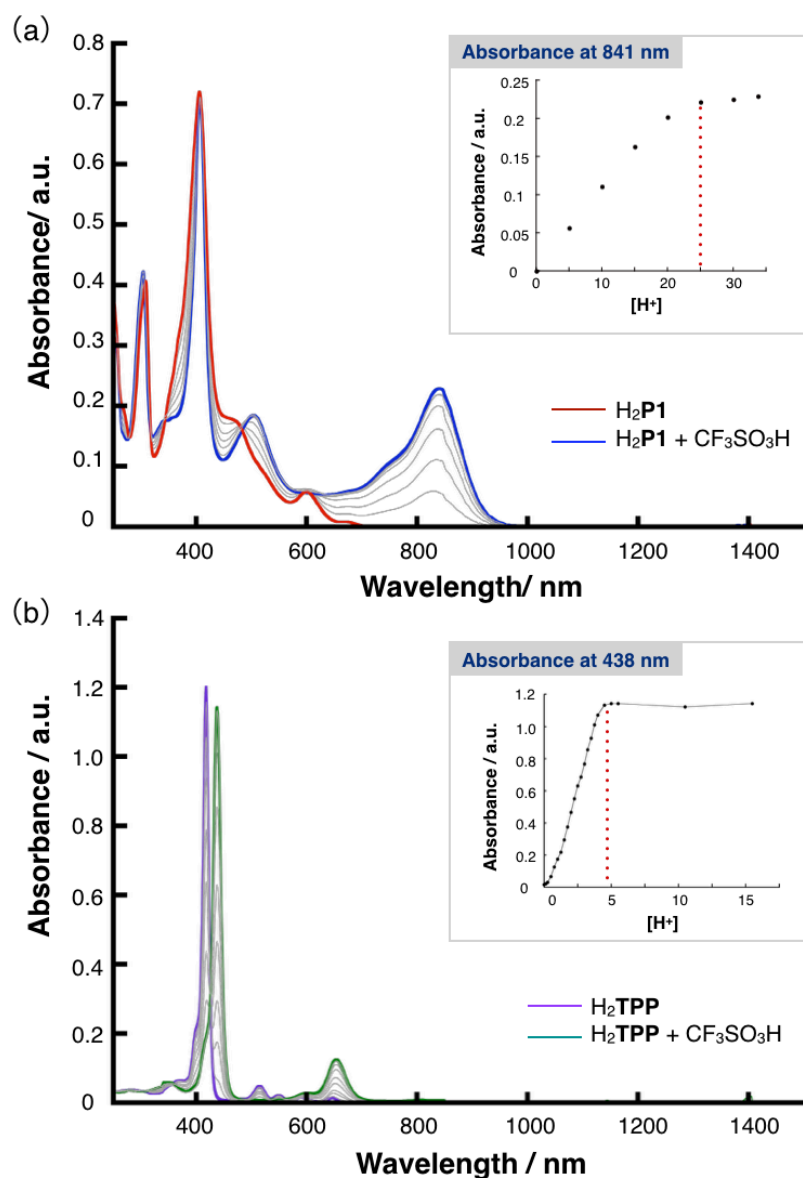
Figure S7. DPVs of carbazole derivative, C1 and H<sub>2</sub>P1.

Table S3. Electrochemical properties of H<sub>2</sub>P1, H<sub>4</sub>P1<sup>2+</sup>, H<sub>2</sub>TPP, and H<sub>4</sub>TPP<sup>2+</sup>.<sup>a</sup>

Compd.	$E_{ox,2}$	$E_{ox,1}$	$E_{red,1}$	$E_{red,2}$
H <sub>2</sub> P1	0.78	0.58	-1.38	-1.81
H <sub>2</sub> TPP	0.85	0.53	-1.69	-1.97
H <sub>4</sub> P1 <sup>2+</sup>	0.83	0.64	-0.61	-
H <sub>4</sub> TPP <sup>2+</sup>	-	-	-1.00 <sup>b</sup>	-

[a] Potentials [V] vs. ferrocene/ferrocenium ion. 0.1 M <sup>n</sup>Bu<sub>4</sub>NPF<sub>6</sub> at 20 °C and a scan rate of 100 mVs<sup>-1</sup>. [H<sub>2</sub>P1] = [H<sub>4</sub>P1<sup>2+</sup>] = 400 μM, working electrode, glassy carbon; counter electrode, Pt wire; reference electrode, Ag/AgCl in CH<sub>3</sub>CN. [b] Ref. [6].

## 6. Photometric titration of trifluoromethanesulfonic acid against H<sub>2</sub>P1 and H<sub>2</sub>TPP



**Figure S8.** UV-vis absorption spectra of H<sub>2</sub>P1 and H<sub>2</sub>TPP titrated with TFSA. (a) [H<sub>2</sub>P1] = 5.0 μM in 50:1 (v/v) CHCl<sub>3</sub>:CH<sub>3</sub>CN at 293 K. Inset, plot of absorbance at 841 nm as a function of [H<sup>+</sup>]/[H<sub>2</sub>P1]. (b) [H<sub>2</sub>TPP] = 2.5 μM in 50:1 (v/v) CHCl<sub>3</sub>:CH<sub>3</sub>CN at 293 K. Inset, plot of absorbance at 438 nm as a function of [H<sup>+</sup>]/[H<sub>2</sub>TPP].

## 7. Theoretical calculations

The molecular structures of  $\text{H}_2\text{P1}$  and  $\text{H}_4\text{P1}^{2+}$  were optimized by the density functional theory (DFT) method at the B3LYP/6-31G\* level of theory, under a solvent ( $\text{CHCl}_3$ ) condition with a polarizable continuum model (PCM) using the integral equation formalism variant (IEFPCM). The optimized structures were confirmed that they do not have imaginary frequencies by normal mode analyses. Excited states (S1 – S70) of those molecules were examined at the optimized geometry by the time-dependent DFT (TD-DFT) calculations using B3LYP/6-31G\*, under the solvent condition ( $\text{CHCl}_3$ ). All calculations were performed by Gaussian 09 program package.<sup>7</sup>

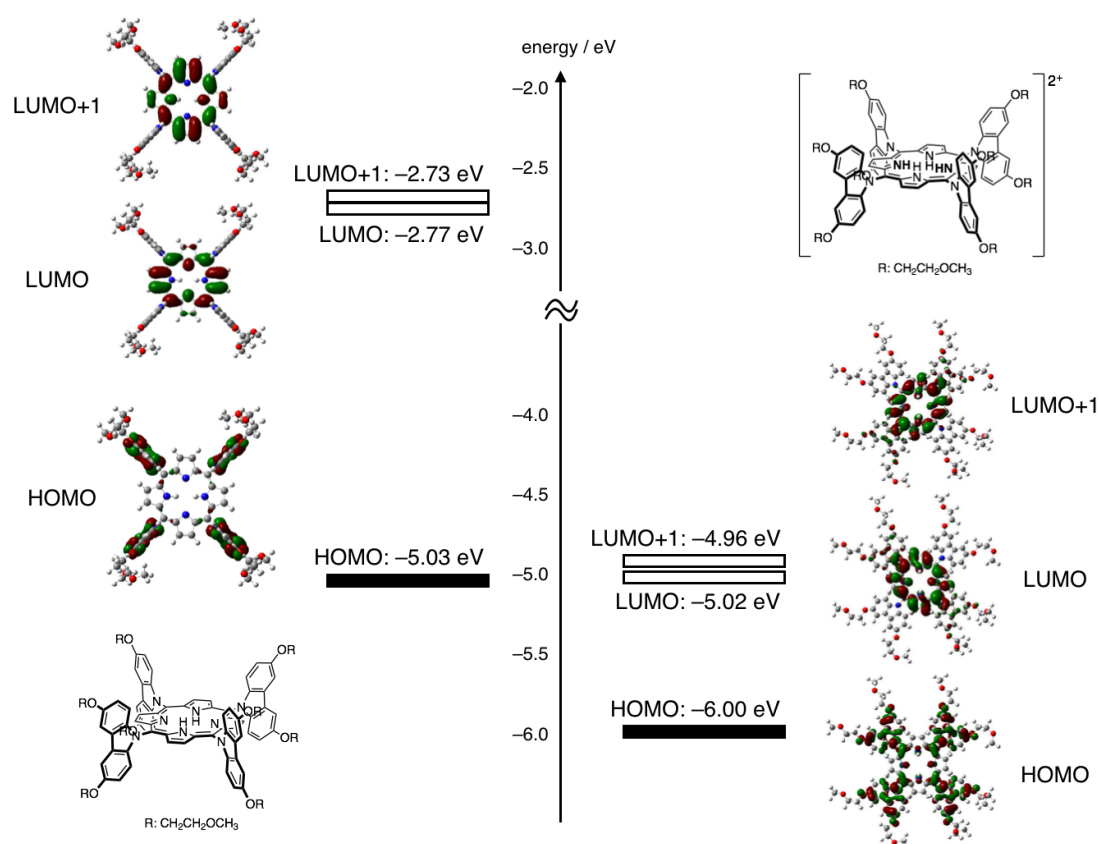


**Figure S9.** Frontier molecular orbitals and their energy levels of  $\text{H}_2\text{P1}$  and  $\text{H}_4\text{P1}^{2+}$  at the B3LYP/6-31G\* level of theory.

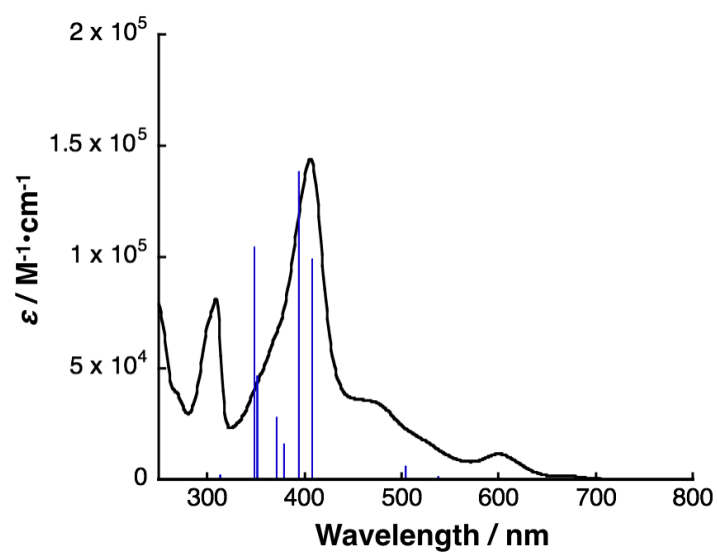


**Figure S10.** Oscillator strengths (blue Bars) obtained by the TD DFT calculation of H<sub>2</sub>P1 at the B3LYP/6-31G\* level of theory and the observed UV-vis absorption spectrum (black line) of H<sub>2</sub>P1.

**Table S4.** Calculated dominant excitations for the optimized geometry of H<sub>2</sub>P1.

Dominant excited state	Transition energy / eV (nm)	Dominant transitions	Oscillator strength $f$
S13	2.31 (538 nm)	HOMO-6→LUMO (80%)	0.0172
S18	2.46 (504 nm)	HOMO-9→LUMO+1 (51%) HOMO-8→LUMO (35%)	0.0625
S19	3.04 (407 nm)	HOMO-9→LUMO (40%) HOMO-8→LUMO+1 (30%)	1.0328
S20	3.15 (394 nm)	HOMO-9→LUMO+1 (39%) HOMO-8→LUMO (36%)	1.4464

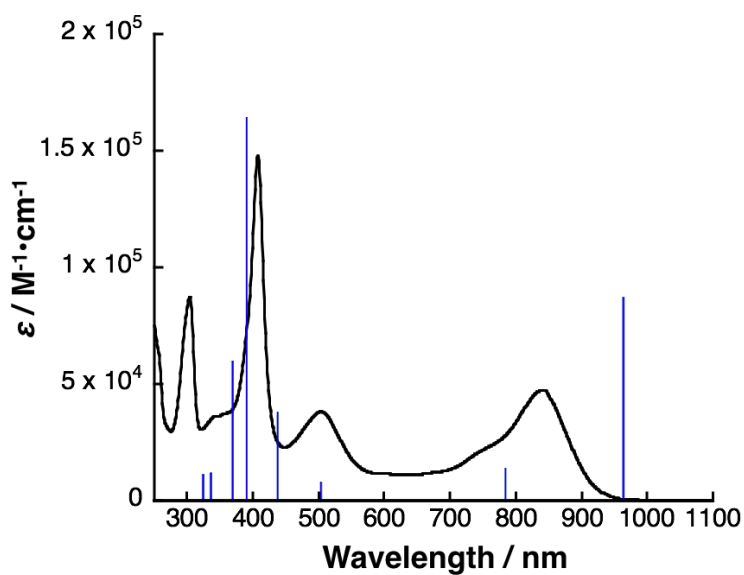


**Figure S11.** Oscillator strengths (blue Bars) obtained by the TD DFT calculation of  $\text{H}_4\text{P1}^{2+}$  at the B3LYP/6-31G\* level of theory and the observed UV-vis absorption spectrum (black line) of  $\text{H}_4\text{P1}^{2+}$ .

**Table S5.** Calculated dominant excitations for the optimized geometry of  $\text{H}_4\text{P1}^{2+}$ .

Dominant excited state	Transition energy / eV (nm)	Dominant transitions	Oscillator strength $f$
S3	1.29 (963 nm)	HOMO-1→LUMO (35%) HOMO-1→LUMO+1 (61%)	0.3634
S13	1.58 (783 nm)	HOMO-5→LUMO (35%) HOMO-4→LUMO (60%)	0.0588
S26	2.47 (503 nm)	HOMO-11→LUMO+1 (38%) HOMO-10→LUMO (19%)	0.0334
S45	2.84 (437 nm)	HOMO-2→LUMO+2 (79%)	0.1541
S51	3.18 (390 nm)	HOMO-21→LUMO+1 (29%)	0.6856

## 8. References

- 1). T. Higashino, Y. Fujimori, K. Sugiura, Y. Tsujii, S. Ito, H. Imahori, *J. Porphr. Phthalocyanines*, 1999, **19**, 99-116.
- 2). (a) K. Wakita, *Yadokari-XG*, Program for Crystal Structure Analysis; 2000. (b) C. Kabuto, S. Akine, E. Kwon, *J. Cryst. Soc. Jpn.* 2009, **51**, 218–224.
- 3). A. L. Spek, *J. Appl. Crystallogr.* 2003, **36**, 7–13.
- 4). L. A. Plaza, J. Chojnacki, *Acta Cryst.* 2012, **C68**, m24-m28.
- 5). N. C. Maiti, M. Ravikanth, *J. Chem. Soc., Faraday Trans.*, 1996, **92**, 1095–1100.
- 6). Y. Cui, L. Zeng, Y. Fang, J. Zhu, C. H. Devillers, D. Lucas, N. Desbois, C. P. Gros, K. M. Kadish, *ChemElectroChem*, 2016, **3**, 228–241.
- 7). Gaussian 09 revision C01, M. J. Frisch, G. W. Trucks, H. B. Schlegel, G. E. Scuseria, M. A. Robb, J. R. Cheeseman, G. Scalmani, V. Barone, B. Mennucci, G. A. Petersson, H. Nakatsuji, M. Caricato, X. Li, H. P. Hratchian, A. F. Izmaylov, J. Bloino, G. Zheng, J. L. Sonnenberg, M. Hada, M. Ehara, K. Toyota, R. Fukuda, J. Hasegawa, M. Ishida, T. Nakajima, Y. Honda, O. Kitao, H. Nakai, T. Vreven, J. A., Jr. Montgomery, J. E. Peralta, F. Ogliaro, M. Bearpark, J. J. Heyd, E. Brothers, K. N. Kudin, V. N. Staroverov, R. Kobayashi, J. Normand, K. Raghavachari, A. Rendell, J. C. Burant, S. S. Iyengar, J. Tomasi, M. Cossi, N. Rega, M. J. Millam, M. Klene, J. E. Knox, J. B. Cross, V. Bakken, C. Adamo, J. Jaramillo, R. Gomperts, R. E. Stratmann, O. Yazyev, A. J. Austin, R. Cammi, C. Pomelli, J. W. Ochterski, R. L. Martin, K. Morokuma, V. G. Zakrzewski, G. A. Voth, P. Salvador, J. J. Dannenberg, S. Dapprich, A. D. Daniels, Ö. Farkas, J. B. Foresman, J. V. Ortiz, J. Cioslowski, D. J. Fox, Gaussian, Inc., Wallingford CT, 2009.